INL/CON-19-56983-Revision-0

CP-DSSS: A Novel Waveform for Multiple Access in IoT

May 2020

Changing the World's Energy Future

Stephen Jenkins, Brent A. Kenney, Arslan J Majid, Hussein Moradi, Behrouz Farhang-Boroujeny

INL/CON-19-56983-Revision-0

CP-DSSS: A Novel Waveform for Multiple Access in IoT

Stephen Jenkins, Brent A. Kenney, Arslan J Majid, Hussein Moradi, Behrouz Farhang-Boroujeny

May 2020

Idaho National Laboratory
Idaho Falls, Idaho 83415

http://www.inl.gov

Prepared for the
U.S. Department of Energy
Under DOE Idaho Operations Office
Contract DE-AC07-05ID14517

CP-DSSS: A Novel Waveform for Multiple Access in IoT

Stephen N. Jenkins*, Brent A. Kenney* Arslan J. Majid†, Hussein Moradi†, and Behrouz Farhang-Boroujeny*
*Electrical and Computer Engineering Department, University of Utah, Salt Lake City, Utah, USA
†Idaho National Laboratory, Salt Lake City, Utah, USA

***Abstract*—Cyclic prefix direct sequence spread spectrum (CP-DSSS) is a novel waveform that positions itself well as a secondary network to relieve the congested wireless spectrum. The underlying structure of CP-DSSS allows for efficient and effective multi-access capabilities through frequency and time division schemes. The sum-rate capacity of the system is maximized when the spectrum is divided and allocated to users with the best signal-to-noise (SNR) ratio for the given channel slice. We propose an algorithm for dividing and allocating portions of the spectrum to multiple users with the final goal of maximizing the sum-rate capacity of the network. We also propose and develop a precoding/equalization technique that reduces the length of the channel impulse response. This, when used along with a matched filter detector, leads to a noticeable improvement in the sum-rate capacity of the network.**

***Index Terms*—CP-DSSS, cyclic prefix direct sequence spread spectrum, femtocell, 5G, 6G, LTE, IoT, mMTC, NG-RAN**

I. Introduction

Cyclic prefix direct sequence spread spectrum is a new waveform that has recently been proposed [1], [2] as a two-tier waveform to alleviate the congested spectrum in the Internet of Things (IoT) paradigm. CP-DSSS is a versatile waveform that provides a variable rate, low interference solution as a femtocell network waveform to meet key next generation radio access network (NG-RAN) objectives, such as massive machine type communications (mMTC) and ultra-reliable low-latency communications (URLLC). CP-DSSS has also been shown to achieve similar capacity results when compared to orthogonal frequency division multiple access (OFDMA) [3]. Connection density has been identified by 3GPP as a key performance indicator (KPI) for mMTC use cases with an expected increase in connection density to $1,000,000$ connected devices per km^2 [4]. With this fore-casted increase in connected devices, complementing methodologies need to be explored in order to satisfy the additional demand on the primary network.

It has been shown that CP-DSSS matches the capacity of OFDM when using the same precoding methods such as equal power (EP) and water-filling (WF) [3]. In CP-DSSS, all data symbols go through the same channel allowing for long, capacity-achieving codewords, in contrast to OFDMA, where distinct codewords are applied to different subcarriers to allow for variable rate and power allocations. Given that typical packet lengths in OFDM symbols/frames is limited to a small number (seven or fourteen in LTE), there will not be a sufficient codeword length in each sub-carrier channel for approaching the predicted capacity [3].

In this paper, we propose CP-DSSS as a multi-access solution to serve the increased number of users. This new waveform provides the flexibility to be divided between users along time and frequency resources in a similar manner to OFDMA methods for the LTE network [5]. The time synchronization signal employed by the primary network may also serve the secondary network and facilitate synchronization among femtocell devices. To service all users in a femtocell, we propose using a combined frequency division multiple access (FDMA) and time division multiple access (TDMA) approach. Each user will be paired with other user(s) that have complementing spectrum and capacity requirements.

The objective of this paper is to develop an FDMA method to sub-divide the spectrum between a certain number of users and show that, for a given time slot, the capacity for multiple users exceeds that of a single user occupying the full spectrum in a TDMA scheme. This approach will constrain each user slice to be a contiguous set of frequency bins, with the ability to wrap in the base-band channel, and have equal bandwidth across users in the given time slot. We use a simple, sum power utility function to allocate the slices of spectrum to distinct users to maximize the received power across their respective channels. It follows that this utility function then maximizes the sum-rate capacity experienced by the end users in the system. To divide up the spectrum, we utilize a well established channel truncation method [6], [7] to design a precoder matrix that reduces the effective channel length, band-limits a user's signal, and reduces receiver complexity in the end user equipment.

This paper is organized as follows. A summary of the CP-DSSS waveform will be presented in Section II. The FDMA method, using an exhaustive search approach to allocate spectrum to each user with the objective of maximizing the sum-rate capacity of the system, is developed in Section III. A channel truncation method with the goal of increasing the sum rate capacity is presented in Section IV. This algorithm also

This manuscript has in part been authored by Battelle Energy Alliance, LLC under Contract No. DE-AC07-05ID14517 with the U.S. Department of Energy. The United States Government retains and the publisher, by accepting the paper for publication, acknowledges that the United States Government retains a nonexclusive, paid-up, irrevocable, world-wide license to publish or reproduce the published form of this manuscript, or allow others to do so, for United States Government purposes. **STI Number: INL/CON-19-56983.**

allows for reduced complexity in the receiver and serves to band-limit each user's signal to reduce inter-user interference in the system. Finally, in Section V, we will detail some simulation results that compare CP-DSSS multi-access techniques in relation to capacity. The concluding remarks of this paper will be presented in Section VI.

Throughout the paper, the following notations are adhered to. Scalar variables are denoted by lowercase nonbold letters. Lowercase bold letters are used to refer to column vectors. Matrices are denoted by upper-case bold letters. The superscripts 'T' and 'H' denote transpose and Hermitian, respectively.

II. CP-DSSS Waveform Summary

The authors in [1] provided details of the CP-DSSS waveform spreading and despreading. A summary of the waveform behavior is presented here for completeness. The spreading sequences used by CP-DSSS are from the family of Zadoff-Chu (ZC) sequences, which have the property of orthogonality between cyclically shifted versions of the same sequence. Let the vector $\mathbf{z}_{(0)}$ represent a ZC sequence of length N scaled to unit power (i.e., $\mathbf{z}_{(0)}^{\mathrm{H}}\mathbf{z}_{(0)} = 1$), where the subscript references the size of the cyclic shift. Since each cyclic shift of $\mathbf{z}_{(0)}$ is orthogonal to the other $N-1$ cyclic shifts, there is a potential of modulating N symbols, one on each of the cyclically shifted ZC vectors. We define the spreading matrix $\mathbf{Z}$ as

$$\mathbf{Z} = \begin{bmatrix}\mathbf{z}_{(0)} & \mathbf{z}_{(1)} & \ldots & \mathbf{z}_{(N-2)} & \mathbf{z}_{(N-1)}\end{bmatrix}. \quad (1)$$

The corresponding despreading matrix is $\mathbf{Z}^{\mathrm{H}}$, since $\mathbf{Z}^{\mathrm{H}}\mathbf{Z} = \mathbf{I}$; the superscript 'H' denotes Hermitian. An important property of $\mathbf{Z}$ and $\mathbf{Z}^{\mathrm{H}}$ is that they are circulant matrices, hence, their multiplication by vectors of length N can be implemented in a computationally efficient means by using the Fast Fourier Transform (FFT) and Inverse Fourier Transform (IFFT), resulting in complexity of $\mathcal{O}(N\log N)$ instead of $\mathcal{O}(N^2)$.

The transmitted signal is formed by multiplying the spreading matrix by a vector $\mathbf{s}$ of N symbols and taking a duplicate of the last N_{cp} samples to be transmitted first as a cyclic prefix (CP). The length of N_{cp} must be greater than or equal to the maximum delay spread of the channel in order to preserve the properties of circular convolution as in OFDM. Accordingly, after removing the CP at the receiver input, we get the length N vector

$$\mathbf{y} = \mathbf{HZs} + \mathbf{v} \quad (2)$$

where $\mathbf{H}$ is the circulant channel matrix. $\mathbf{H}$ is formed by taking the channel impulse response, $\mathbf{h}$, of length L_h, appending $N - L_h$ zeros to it to form $\mathbf{h}_{(0)}$, and then taking cyclic shifts of $\mathbf{h}_{(0)}$ to create $\mathbf{H} = \begin{bmatrix}\mathbf{h}_{(0)} & \mathbf{h}_{(1)} & \ldots & \mathbf{h}_{(N-2)} & \mathbf{h}_{(N-1)}\end{bmatrix}$, as was done to form $\mathbf{Z}$.

To despread the received signal, $\mathbf{y}$ is left multiplied by $\mathbf{Z}^{\mathrm{H}}$, leading to

$$\tilde{\mathbf{y}} = \mathbf{Hs} + \tilde{\mathbf{v}}, \quad (3)$$

where $\tilde{\mathbf{v}} = \mathbf{Z}^{\mathrm{H}}\mathbf{v}$ and it has been noted since $\mathbf{Z}$, $\mathbf{Z}^{\mathrm{H}}$ and $\mathbf{H}$ are circulant matrices, $\mathbf{Z}^{\mathrm{H}}\mathbf{HZ} = \mathbf{HZ}^{\mathrm{H}}\mathbf{Z} = \mathbf{H}$. Moreover, since $\mathbf{Z}^{\mathrm{H}}$ is a unitary matrix $\tilde{\mathbf{v}}$ holds the same statistics as $\mathbf{v}$.

A. Detection/Precoding

In the uplink, the detection of the symbol vector $\mathbf{s}$ may be obtained through pre-multiplication of $\tilde{\mathbf{y}}$ by a linear detector matrix $\mathbf{G}$. That is,

$$\hat{\mathbf{s}} = \mathbf{GHs} + \tilde{\mathbf{v}}' \quad (4)$$

where $\tilde{\mathbf{v}}' = \mathbf{G}\tilde{\mathbf{v}}$. Since $\mathbf{H}$ is a circulant matrix, a choice of circulant $\mathbf{G}$ also turns out to be an effective design. A design of $\mathbf{G}$ is deferred to Section IV. At this point, we simply remind the reader that a good design of $\mathbf{G}$ satisfies the approximate identity $\mathbf{GH} \approx \mathbf{I}$.

In the downlink, on the other hand, to keep the complexity of UEs/devices low, instead of adopting a linear detector at the receiver side, we resort to a precoder at the FGW. To this end, we note that since $\mathbf{H}$ (by waveform construction) and $\mathbf{G}$ (by design) are circulant matrices, $\mathbf{GH} = \mathbf{HG}$. Considering this identity, one may propose that the data vector $\mathbf{s}$ be replaced by the precoded vector $\mathbf{Gs}$, before spreading. This leads to the despread received signal vector

$$\tilde{\mathbf{y}} = \mathbf{HGs} + \tilde{\mathbf{v}} \quad (5)$$

which in light of the identity $\mathbf{GH} \approx \mathbf{I}$ gives an estimate of $\mathbf{s}$ without any further processing.

B. Symbol Rate Reduction

Although capacity is generally maximized when N symbols are sent per CP-DSSS frame, there are advantages to reducing the symbol rate. For example, if, for a given SNR, the capacity calculation shows that the number of bits per symbol is very low (e.g., ≤ 0.1), then an FEC scheme of high complexity must be used to encode the data, resulting in higher receiver complexity. Reducing the symbol rate allows more power to be transmitted per symbol, while still maintaining the same signal to noise ratio (SNR). Consequently, higher bit to symbol ratios can be used that are within the range of today's FEC schemes (e.g., 0.2 to 0.83 for 5G NR. [8]). Another reason for reducing the symbol rate in CP-DSSS is to spread out the symbols, so that there is less impact from inter-symbol interference (ISI).

As described in [3], symbol rate reduction is accomplished by forming an expander matrix, $\mathbf{E}_L$, which is based on the symbol reduction factor, L. The form of $\mathbf{E}_L$ can be described as an identity matrix of dimension N/L (i.e. $\mathbf{I}_{N/L}$) that has been up-sampled in the vertical dimension by a factor of L. In other words, after each row of $\mathbf{I}_{N/L}$, $L-1$ rows of zeros are inserted, resulting in an $N \times N/L$ matrix. When symbol reduction and precoding are employed (i.e., in the case of downlink), the received signal takes the form

$$\tilde{\mathbf{y}} = \mathbf{HGE}_L\mathbf{s} + \tilde{\mathbf{v}}, \quad (6)$$

where the $\mathbf{s}$ has N/L symbols and each symbol is scaled up by $\sqrt{L}$.

III. CP-DSSS Multi-access System Model

In the multi-access system model for CP-DSSS operating in a femtocell environment, we will have a total of M users sharing the same wide-band spectrum, communicating with a single base station called femtocell gateway (FGW). The FGW will serve as the connection to a primary network, such as LTE. Using a combined FDMA/TDMA approach, a subset of K users will be communicating with the FGW, through FDM, in each time division slot. It naturally follows that the system will need $\lceil M/K \rceil$ time slots for the TDMA mode to service all users in a proportional fair manner.

The problem of pairing subsets of K users that will use the sub-divided spectrum concurrently, is a $\binom{M}{K}$ combinatorial problem that grows exponentially in complexity with an increased number of users. Additional use cases that require additional quality of service (QoS) considerations, such as, equal sum-rate capacity or demand based proportional capacity, make this problem a good candidate for machine learning (ML) and artificial intelligence (AI). Deriving optimal solutions will become very expensive as the number of connected devices grow, so sub-optimal, but tractable, solutions for embedded platforms is desirable. These additional constraints will be addressed in our future research.

This paper details an exhaustive search approach for allocating spectrum to K users, utilizing the same TDMA slot, by developing a cost function to look at each respective user's channel and allocate portions of spectrum that maximizes the received sum-power of all users at the FGW, in the uplink case, and at the end user equipment (UE), in the downlink case. The end objective of this cost function is to find an optimal frequency division among users, under certain constraints, that maximizes the overall sum-rate capacity of the system. We follow the frequency allocation scheme shown in Fig. 1, where the wideband channel is allocated to K users in contiguous portions of spectrum with the ability to wrap in the base-band channel.

Mathematically, the cost function for optimizing channel allocation for each user is formulated as:

$$\arg\max_{\ell,\kappa} \sum_{k} \sum_{n \in S_{\kappa}^{(\ell)}} |H_k(n)|^2$$

$$\begin{aligned}
\text{subject to} \quad & |S_1^{(\ell)}| = |S_2^{(\ell)}| = \ldots = |S_K^{(\ell)}| \\
& \ell \leq \lfloor N/K \rfloor \\
& S_1^{(\ell)} \neq S_2^{(\ell)} \neq \ldots \neq S_K^{(\ell)} \\
& S_k^{(\ell)} \quad \text{is a contiguous set.}
\end{aligned} \tag{7}$$

In (7), k is the user index, n is the frequency bin index, $S_{\kappa}^{(\ell)}$ indicates the set of frequency bin indices that are allocated to user κ, and κ is searched over all user indices of the set $\{1, 2, \cdots, K\}$. Also, in (7), $|S_{\kappa}^{(\ell)}|$ indicates the cardinality of $S_{\kappa}^{(\ell)}$. The specific objective of this optimization equation is to find the correct permutation of users κ and frequency offset ℓ that gives the maximum power received at the FGW, in the uplink case, or at the end UEs, in the downlink case, through the combined frequency divided channels, under the constraints specified.

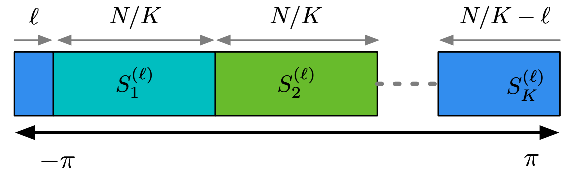

Fig. 1. Baseband channel allocation method where K is the number of users, N is the number of frequency bins in the wideband spectrum (equivalent to sub-carriers in OFDM), S_k is the set of frequency bins allocated to user k, and ℓ is the frequency offset of the system to allow for maximum received power.

The constraints for the optimization equation in (7) facilitate the precoder design that will be discussed in Section IV. The first constraint states that each user is granted an equivalent number of frequency resources, $S_k^{(\ell)}$. The second constraint limits the frequency offset allowed for the combined channel slices. It follows that a frequency shift/offset greater than $\lfloor N/K \rfloor$ would simply be a different permutation in κ. Additionally, the frequency offset ℓ is a system wide optimization, indicating that each user employs the same shift to maximize their channel state. The third constraint says that frequency resources must be mutually exclusive among users. Our future research will look into the possibilities of widening the transition bands and allow some frequency reuse to take advantage of the robust inter-user interference mitigation provided by the CP-DSSS structure. The fourth constraint states that each set of frequency resources granted to a user must be in a contiguous set. This constraint reduces the complexity of filter design while consideration for non-contiguous frequency assignments, to further the optimization of the wireless channel, will be considered at later date.

The exhaustive search method detailed in (7) iterates over all permutations in the set of K users and looks at the channel state information of each user's spectrum, and finds the sub-channel allocation for the best permutation of users, along with the frequency offset, that gives the maximum power received. Once the users bands are selected, a set of precoders that band-limit the signals of different users should be designed. This is the subject of the next section.

IV. Equalizer Design, Detection, and Precoding

To employ the FDMA scheme, we need a filter design to separate the users into their allotted slice of the wireless channel. The brick wall filter, also known as an equal power filter, is a good first choice as it has a flat pass-band and ideal roll-off. The drawback of the brick wall filter is that it extends the length of the channel due to the steep roll-off of the transition bands, and as a result, introduces additional ISI into the system, thus limiting the overall sum-rate capacity. This drawback can be resolved through a channel truncation design that is introduced here.

The channel truncation involves optimizing the coefficients of a linear equalizer, for a given channel, so that when it is applied to a transmitted/received signal, the effective impulse response of the system is reduced in length (memory). The original motivation of this equalizer design was to reduce the complexity of iterative decoding methods that become exponentially complex with increased length of the channel [6]. Additional methods have built on this original idea by reducing the computational complexity of finding the optimum equalizer coefficients through iterative algorithms [7].

In this paper, we propose a design strategy that constructs the detector/precoder matrix $\mathbf{G}$ as the multiplication of an equalizer matrix $\mathbf{G}_\mathrm{e}$ and a matched filter matrix $\mathbf{D}^\mathrm{H}$ whose details are given in the sequel.

The equalizer matrix $\mathbf{G}_\mathrm{e}$ is a circulant matrix, that when multiplied by the channel matrix $\mathbf{H}$, the result is a circulant matrix corresponding to an effective channel which is truncated to a specific length. Mathematically, this may be represented by saying that $\mathbf{G}_\mathrm{e}\mathbf{H} \approx \mathbf{D}$ where $\mathbf{D}$ is a circulant matrix in which only the first L elements of its first column are non-zero. At the same time, $\mathbf{G}_\mathrm{e}$ is designed to concentrate on the specific band that belongs to each UE. To accomplish this goal, we add two terms to the cost function, originally suggested in [6], to minimize the stop-band frequencies and to flatten the response in the pass-band. The cost function that we propose for deriving the equalizer coefficients $\{g_\mathrm{e}(n); \quad n = 0, 1, \cdots, N-1\}$ (the first column of $\mathbf{G}_\mathrm{e}$) and the desired impulse response of the truncated channel $\{d(n); \quad n = 0, 1, \cdots\}$ (the non-zero elements of the first column of $\mathbf{D}$) is

$$J = \sum_{n\in\psi} |e(n)|^2 + \gamma \sum_{f_i\in\varphi} |G_\mathrm{e}(f_i)|^2 + \alpha \sum_{f_i\in\zeta} |G_\mathrm{e}(f_i)|^2 \tag{8}$$

where $e(n) = g_\mathrm{e}(n) * h(n) - d(n)$, the frequency response of the equalizer is defined as

$$G_\mathrm{e}(f) = \sum_n g_\mathrm{e}(n) e^{-j2\pi f n} \tag{9}$$

$\psi = [0\ 1\ \cdots\ N-1]^\mathrm{T}$, φ is a set of frequencies in the desired stop-band, ζ is a sub-set of frequencies at the center of the pass-band, and γ and α are scaling factors for the stop-band and pass-band frequencies, respectively. Scaling factors are used in the minimization function to proportionally remove energy from the corresponding frequency bins. The scaling factor α allows us to flatten the pass-band and decrease the width of the transition-band. When $\alpha = 0$, the eigenfilter design allows for wide transition bands, and thus provides poor response at the edges of the pass-band. This reduces the obtained transmission capacity. We want to approximate the brick wall filter while minimizing the amount of ISI introduced. To this end, we apply an $\alpha \ll \gamma$, which acts to flatten the response in the pass-band. The precoder coefficients and desired response are determined through minimizing J. To prevent the trivial solution of $g_\mathrm{e}(n) = d(n) = 0$, we apply the constraint $\sum_n |d(n)|^2 = 1$.

To facilitate the derivations, we define the following:

$$\mathbf{e} = \mathbf{H}\mathbf{g}_\mathrm{e} - \mathbf{d} \tag{10}$$

where $\mathbf{g}_\mathrm{e}$ and $\mathbf{d}$ are the first columns of $\mathbf{G}_\mathrm{e}$ and $\mathbf{D}$, respectively. To further simplify the notation, we define the composite matrix $\mathbf{C} \triangleq \begin{bmatrix} \mathbf{H} \\ \mathbf{F}_\varphi \\ \mathbf{F}_\zeta \end{bmatrix}$ while extending the desired response $\mathbf{d}$ by appending extra zeros so the dimensions will be compatible for matrix operations. The matrices $\mathbf{F}_\varphi$ and $\mathbf{F}_\zeta$ contain the relevant Fourier coefficients in (9). With these definitions, one finds that the cost function J may be written in the compact form

$$J = \mathbf{e}_\mathbf{c}^\mathrm{H}\mathbf{e}_\mathbf{c} \tag{11}$$

where $\mathbf{e}_\mathbf{c} = \mathbf{C}\mathbf{g}_\mathrm{e} - \mathbf{d}$.

We note that the minimization of J is a least-squares problem that can be solved by applying the principle of orthogonality (see Section 3.3 in [9]), so that $\mathbf{C}^\mathrm{H}\mathbf{e}_\mathbf{c} = \mathbf{0}$. This leads to the well known *Weiner-Hopf* equation

$$(\mathbf{C}^\mathrm{H}\mathbf{C})\mathbf{g}_\text{e,opt} = \mathbf{C}^\mathrm{H}\mathbf{d}. \tag{12}$$

We further note that the desired truncated response $\mathbf{d}$ may take non-zero values for a subset of its elements, to keep the equalized/precoded channel to the desired length. Let $\mathbf{d}'$ denote the vector whose elements are non-zero elements in $\mathbf{d}$, and $\mathbf{C}'$ be the matrix with the corresponding subset of rows of $\mathbf{C}$ that correspond to $\mathbf{d}'$. This leads to

$$\mathbf{g}_\text{e,opt} = (\mathbf{C}^\mathrm{H}\mathbf{C})^{-\mathbf{1}}(\mathbf{C}')^\mathrm{H}\mathbf{d}' \tag{13}$$

For $\mathbf{g} = \mathbf{g}_\text{e,opt}$,

$$J(\mathbf{g}_\text{e,opt}) = (\mathbf{d}')^\mathrm{H}\mathbf{Q}\mathbf{d}' \tag{14}$$

where $\mathbf{Q} = \mathbf{I} - \mathbf{C}'(\mathbf{C}^\mathrm{H}\mathbf{C})^{-1}(\mathbf{C}')^\mathrm{H}$. With the constraint $\sum_n |d(n)|^2 = (\mathbf{d}')^\mathrm{H}\mathbf{d}' = 1$, it follows that $J(\mathbf{g}_\text{e,opt})$ is minimized when $\mathbf{d}'$ is selected to be the eigenvector attached to the minimum eigenvalue of the matrix $\mathbf{Q}$ [6].

Next, consider the case where the symbol rate reduction method discussed in Section II-B has been applied and $\mathbf{G}_\mathrm{e}$ and $\mathbf{D}$ are optimized and the same symbol reduction factor/truncated channel length L has been used.

In the case of uplink, the received signal at FGW, after despreading, finds the form of

$$\tilde{\mathbf{y}} = \mathbf{H}\mathbf{E}_L\mathbf{s} + \tilde{\mathbf{v}}. \tag{15}$$

Here, a linear detector that may be applied to $\tilde{\mathbf{y}}$ to extract an estimate of $\mathbf{s}$ is defined as

$$\hat{\mathbf{s}} = \mathbf{E}_L^\mathrm{H}\mathbf{G}\tilde{\mathbf{y}} = \mathbf{E}_L^\mathrm{H}\mathbf{G}\mathbf{H}\mathbf{E}_L\mathbf{s} + \tilde{\mathbf{v}}' \tag{16}$$

where $\mathbf{G} = \mathbf{D}^\mathrm{H}\mathbf{G}_\mathrm{e}$. In (16), given the construction of the matrix $\mathbf{G}$, one can show that $\mathbf{E}_L^\mathrm{H}\mathbf{G}\mathbf{H}\mathbf{E}_L \approx \mathbf{I}$ and, hence, argue that (16) gives a good estimate of $\mathbf{s}$.

In the case of downlink, on the other hand, following the same logic as in Section II-A, the transmit signal is $\mathbf{G}\mathbf{E}_L\mathbf{s}$ and the channel premultiply this by $\mathbf{H}$. When a number of UEs use the same channel in an FDMA manner, each UE has to extract the portion of the transmission band that belongs to it. This is done by taking the FFT of the received signal, masking the frequency components that belong to other UEs, and converting the result back to time domain through an IFFT. This filtered result is premultiplied by $\mathbf{E}_L^{\mathrm{H}}$, which is simply a decimation process, to obtain an estimate of the respective data symbols.

V. Results

In this section, we present simulation results to show the performance of the proposed channel allocation and precoder design algorithms. We compare the sum-rate capacity of the system for a single TDMA user over the whole band, with 4x transmit power, and the proposed FDMA scheme with 4 users, transmitting at 1x power, with and without truncation. The analysis is performed in the SNR range that would be allotted to a secondary network. We average the results over 1000 channel realizations for each user. Due to the limited space we only present the results of an uplink case.

In all simulations, we use a randomly generated, tapped-delay line (TDL) channel with power delay profile model A, with a delay rms spread of 30 ns [10]. We use $N = 2048$, a desired channel length and symbol reduction factor $L = 16$. Fig. 2 presents the capacity simulation results for 3 scenarios; (1) A TDMA user that is allowed to use the full time slot and bandwidth resources. We allow the user to transmit at 4x power for equivalent comparison to the FDMA scheme. (2) FDMA with a brick wall filter, and (3) FDMA with the proposed precoder design for channel truncation. The propose precoder design performs about 15% better than the brick wall filter. It is also seen that the FDMA scheme performs better than the single user TDMA scheme by a factor of 1.97 at -20 dB SNR and a factor of 3.16 at 0 dB SNR.

Next, we make an attempt to explain why FDMA outperforms TDMA by a significant margin, particularly as SNR increases. Among other reasons, in order to allow the use of a simple matched filter detector, here, we have chosen to keep data symbols sufficiently apart from each other; $L = 16$ in the example given here. This choice of L has been dictated by the duration of the channel impulse response. We may further note that this duration relates to the time spreading of the channel and, thus, is minimally affected by the transmission bandwidth. Consequently, the same value of L is used in both cases of TDMA and FDMA. As a result, one may note that within one CP-DSSS frame, while the TDMA scheme transmits N/L data symbols, the four users in the FDMA scheme collectively transmit 4 times more symbols. It may thus be concluded that at high SNR, FDMA may offer four times more capacity than TDMA. The plots in Fig. 2 clearly shows this trend of the results.

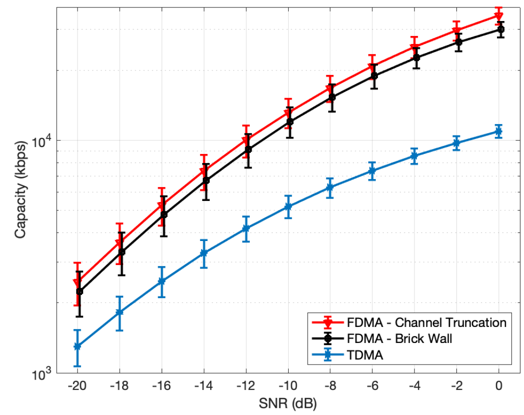

Fig. 2. Comparison of the sum-rate capacity results.

VI. Conclusion

In this paper, we presented the multi-access capabilities of the CP-DSSS waveform. The characteristics of the CP-DSSS waveform, such as variable rate and power distribution, provide significant advantages when used in a FDMA mode. The channel allocation scheme presented finds the optimal slices of spectrum for each user, to maximize the sum-rate capacity of the system. The proposed truncation method derives the optimal detector/precoder coefficients for a band-limiting filter while simultaneously reducing the effective channel length. The presented simulation results showed a significant gain in the sum-rate capacity of the network.

References

[1] A. Aminjavaheri, A. Rezazadehreyhani, R. Khalona, H. Moradi, and B. Farhang-Boroujeny, "Underlay control signaling for ultra-reliable low-latency IoT communications," *2018 IEEE International Conference on Communications Workshops, ICC Workshops 2018 - Proceedings*, pp. 1–6, 2018.

[2] H. Moradi and B. Farhang-Boroujeny, "Underlay Scheduling Request for Ultra-Reliable Low-Latency Communications," in *2019 IEEE 2nd 5G World Forum (5GWF)*. IEEE, sep 2019, pp. 28–33. [Online]. Available: https://ieeexplore.ieee.org/document/8911714/

[3] B. Kenney, S. Jenkins, A. Majid, H. Moradi, and B. Farhang-boroujeny, "Cyclic Prefix Direct Sequence Spread Spectrum Capacity Analysis."

[4] 3GPP and ETSI, "TS 122 261 - V15.5.0 - 5G; Service requirements for next generation new services and markets (Release 15)," Tech. Rep., 2018. [Online]. Available: https://www.etsi.org/deliver/etsi_ts/122200_122299/122261/15.05.00_60/ts_122261v150500p.pdf

[5] Zukang Shen, J. Andrews, and B. Evans, "Adaptive resource allocation in multiuser OFDM systems with proportional rate constraints," *IEEE Transactions on Wireless Communications*, vol. 4, no. 6, pp. 2726–2737, nov 2005. [Online]. Available: http://ieeexplore.ieee.org/document/1545851/

[6] D. D. Falconer and F. R. Magee, "Adaptive Channel Memory Truncation for Maximum Likelihood Sequence Estimation," *Bell System Technical Journal*, vol. 52, no. 9, pp. 1541–1562, 1973.

[7] Farhang-Boroujeny, "Channel memory truncation for maximum likelihood sequence estimation," in *Proceedings of GLOBECOM 95 GLOCOM-95*. IEEE, 1995, pp. 172–176. [Online]. Available: http://ieeexplore.ieee.org/document/502954/

[8] E. Dahlman, S. Parkvall, and J. Skold, *5G NR: the Next Generation Wireless Access Technology*. Elsevier, 2018. [Online]. Available: https://linkinghub.elsevier.com/retrieve/pii/C20170013472

[9] B. Farhang-Boroujeny, "Adaptive filters: Theory and applications," 1999.

[10] 3GPP and ETSI, "TR 138 901 V14.0.0 Study on channel model for frequencies from 0.5 to 100 GHz," Tech. Rep., 2017. [Online]. Available: https://www.etsi.org/deliver/etsi_tr/138900_138999/138901/14.00.00_60/tr_138901v140000p.pdf